

20 **Abstract**

21 Polycyclic aromatic hydrocarbons (PAHs) are considered as priority pollutants because of their
22 high risk to human health. In this paper, we addressed the issue of using hydrotalcite-based
23 nanocomposites as adsorbents of six low molecular weight PAHs (acenaphthene, fluorene,
24 phenanthrene, anthracene, fluoranthene and pyrene) to reduce their negative effects on the
25 environment. A nanocomposite (HT-DDS) was prepared by intercalating the organic anion
26 dodecylsulfate (DDS) in a Mg-Al hydrotalcite (HT), and then characterized using several
27 analytical techniques. A Mediterranean soil was selected for being a high-risk scenario of
28 groundwater contamination by leaching of pollutants. The nanocomposite displayed enhanced
29 affinity for the PAHs in water as compared to carbonate-hydrotalcite (HTCO_3) and its calcined
30 product (HT500), and showed a high irreversibility of the adsorption process (hysteresis
31 coefficient, $H < 0.15$). The results revealed an increase of the pollutants retention in the soil by
32 the addition of the nanocomposite that depended on the nanocomposite application rate and also
33 on the hydrophobicity of each PAH. Accordingly, the use of HT-DDS as an amendment or
34 barrier in contaminated soil is proposed for reducing the mobility of PAHs and, consequently,
35 the adverse effect derived from rapid transport losses of the pollutants to the adjoining
36 environmental compartments.

37

38 *Key words:* adsorption; contaminated soils; hydrotalcite; nanocomposite; polycyclic aromatic
39 hydrocarbons.

40

41

42 **1. Introduction**

43 The nature of Mediterranean soils is strongly influenced by climate conditions, characterized
44 by long periods of drought, together with short, strong, and irregular rainfalls. These
45 characteristics contribute to the creation of natural systems sensitive to degradation, entailing a
46 situation of high risk for chemical pollution of various kinds.

47 A representative group of organic pollutants are the polycyclic aromatic hydrocarbons
48 (PAHs), whose study is prioritized by their great ubiquity, potential bioaccumulation,
49 carcinogenicity, and resistance to biodegradation [1,2]. PAHs are often found in contaminated
50 soils as a mixture of low (2-4 aromatic rings) and high (5 or more aromatic rings) molecular
51 weight compounds, generally owning hydrophobic characteristics and low solubility in water.
52 Nevertheless, low molecular weight PAHs are less hydrophobic and more water soluble than
53 high molecular weight PAHs, and hence can display greater mobility in soils and increased risk
54 of pollution of adjacent aquatic ecosystems. In this work, six PAH compounds (acenaphthene,
55 fluorene, phenanthrene, anthracene, fluoranthene and pyrene) have been selected primarily by
56 their low molecular weight, higher solubility and lower hydrophobicity compared with other
57 chemicals of the same nature.

58 There is growing interest in the study and development of new adsorbents applicable to the
59 remediation of soils as immobilizers and insulating contaminants therein [3,4]. Water
60 contamination by transport of pollutants from the adjacent environmental compartments would
61 involve the application of treatments for decontamination that are usually complicated, lengthy,
62 expensive, and often not feasible. The research of new adsorbents is a strategy to remediate the
63 contamination of water produced by the increase of the anthropogenic activities [5-8]. In
64 addition, application of environmentally friendly adsorbents into natural systems is particularly
65 important to entail minimal environmental impact.

66 Layered double hydroxides (LDHs) are minerals that can be easily synthesized in the
67 laboratory. They consist of positively charged brucite-type layers of mixed divalent (M^{II}) and
68 trivalent (M^{III}) metal hydroxide, $[M^{II}_{1-x}M^{III}_x(OH)_2]^{x+}$, where the positive charge is balanced by
69 exchangeable hydrated anions located in the interlamellar domain ($A_{x/n}^{n-} \cdot mH_2O$) [5,9]. LDHs,

70 also referred to as anionic clays, are considered as very useful materials in diverse fields of
71 application, due to the ease of synthesis, peculiar properties derived from their structure, and
72 wide combination range of the components of both layers and interlayers [6,10].

73 According to their behavior as anion exchangers and their “memory effect” (i.e. recovering
74 of the original layered structure by rehydration of the LDH calcined product), LDHs have good
75 properties as adsorbents for anionic organic pollutants [11-14]. However, the original inorganic
76 composition of these materials gives them a hydrophilic nature. As a result, they usually have a
77 low affinity for non-ionic organic compounds. The intercalation of organic anions in LDHs
78 changes the nature of the surface to hydrophobic, improving the adsorption ability to non-ionic
79 organic compounds. Consequently, these organo/LDHs have applications in a wide range of
80 organic pollution control fields [6,7,15-18].

81 To date, literature on the potential usefulness of organo/LDHs as adsorbents of PAHs from
82 aqueous solution is scarce. Recently, Chuang et al. [19] demonstrated that a Mg/Al (2:1) LDH
83 intercalated with dodecylsulfate (DDS) anions and the bio-surfactant rhamnolipid displayed
84 good adsorbent properties for naphthalene in aqueous solution. However, to our knowledge,
85 there is no published information about the use of LDH-DDS nanocomposites as adsorbents of
86 other PAHs from water or as soil amendments to enhance the PAH retention process in soil.

87 The aim of this work was to prepare and characterize an organo/LDH nanocomposite,
88 consisting of Mg/Al (3:1) LDH or hydrotalcite intercalated with DDS anions. Once synthesized,
89 the most novel aspect of this work lied in the assessment of the removal of six PAHs
90 (acenaphthene, fluorene, phenanthrene, anthracene, fluoranthene and pyrene) from water using
91 the nanocomposite, as well as to determine the effect of its application to a typical
92 Mediterranean soil in the process of retention of such pollutants, as a strategy to reduce their
93 mobility in the soil and decrease their spread through the different environmental compartments.

94

95 **2. Materials and methods**

96 *2.1. PAHs, organic anion and soil*

97 The six PAHs used in this study were supplied by Sigma-Aldrich in powder form and with a
98 purity ranging between 96% and > 99% depending on the compound. Table 1 summarizes the
99 molecular structure and some of the most relevant physicochemical properties of these
100 chemicals [20-22].

101 The organic anion dodecylsulfate (DDS) used for the preparation of the organo/LDH
102 nanohybrid was purchased as soluble sodium salt from Sigma-Aldrich (Spain), with a purity >
103 99%. All the chemicals were used as received without further purification.

104 The soil used in the experiments was a sandy clay loam soil from Coria del Rio (Seville,
105 Spain) and contained no background concentration of the PAHs chosen, as determined by
106 soxhlet extraction for 8 h with dichloromethane [23]. The Mediterranean soil was sampled (0–
107 20 cm), air-dried, sieved (2 mm), and stored at 4°C until used. Soil texture (25% clay, 8% silt,
108 and 67% sand) was determined by sedimentation. The organic carbon content was 0.52% and
109 the pH was 7.2 in a 1:2 (w:w) soil:deionized water mixture.

110

111 *2.2. Preparation and characterization of the organo/LDH*

112 Organo/LDH $[\text{Mg}_3\text{Al}(\text{OH})_8][\text{CH}_3(\text{CH}_2)_{10}\text{CH}_2\text{SO}_4]\cdot n\text{H}_2\text{O}$ was obtained by the coprecipitation
113 method in a N_2 atmosphere and CO_2 -free water. An aqueous solution (100 mL) containing 0.06
114 mol of $\text{Mg}(\text{NO}_3)_2\cdot 6\text{H}_2\text{O}$ and 0.02 mol of $\text{Al}(\text{NO}_3)_3\cdot 9\text{H}_2\text{O}$ (Mg/Al ratio = 3) was added dropwise
115 to an alkaline solution (500 mL) containing 0.16 mol of NaOH and 0.05 mol of sodium
116 dodecylsulfate. The suspension thus obtained was hydrothermally treated at 80 °C for 24 h, and
117 the precipitate washed with CO_2 -free distilled water, and dried at 60 °C. The sample was figured
118 as HT-DDS.

119 For comparison purposes, an inorganic hydrotalcite $[\text{Mg}_3\text{Al}(\text{OH})_8]_2\text{CO}_3\cdot n\text{H}_2\text{O}$ (HTCO₃) was
120 prepared by the coprecipitation method [24], adding dropwise an aqueous solution (100 mL)
121 containing 0.75 mol of $\text{Mg}(\text{NO}_3)_2\cdot 6\text{H}_2\text{O}$ and 0.25 mol of $\text{Al}(\text{NO}_3)_3\cdot 9\text{H}_2\text{O}$ to an alkaline solution
122 (500 mL) containing 2 mol of NaOH and 0.375 mol of Na_2CO_3 . The suspension was subjected

123 to the same process described above. Afterward, an aliquot of the sample was calcined at 500 °C
124 to obtain magnesium aluminum oxide $Mg_3AlO_4.5$ (HT500).

125 HT-DDS and $HTCO_3$ were characterized by different physicochemical techniques.
126 Elemental chemical analysis of Mg and Al was conducted using atomic absorption spectrometry
127 on a Perkin Elmer AA-3100 instrument, after dissolving the samples in a 10% HCl solution.
128 Elemental C, N and S analyses were conducted in a Perkin Elmer 240C analyzer.

129 Powder X-ray diffraction (PXRD) diagrams were collected at room temperature under air
130 conditions, on a Siemens D-5000 instrument with CuK_{α} radiation ($\lambda = 1.54050 \text{ \AA}$) and quartz as
131 an external standard. The Fourier-transform infrared (FT-IR) spectra were obtained with a
132 Perkin Elmer Spectrum One spectrophotometer using the KBr disk technique. One hundred
133 scans were averaged to improve the signal-to-noise ratio, at a nominal resolution of 2 cm^{-1} .

134 The hydration water content was obtained from thermogravimetric (TG) curves recorded on
135 a Setaram Setsys Evolution 16/18 apparatus. The analyses were carried out flowing air from Air
136 Liquide (Spain) and using a heating rate of $5 \text{ }^{\circ}\text{C}/\text{min}$.

137

138 2.3. Adsorption-desorption isotherms

139 The procedure used to study the adsorption of PAHs on HT-DDS, $HTCO_3$ and HT500 was
140 the batch equilibration technique at $20 \pm 2 \text{ }^{\circ}\text{C}$, thus obtaining the corresponding adsorption-
141 desorption isotherms. Duplicate 10 mg adsorbent samples were equilibrated under end-over-end
142 shaking at 52 rpm for 24 h with 10 mL of an aqueous solution containing a mixture of the six
143 PAHs, with individual initial PAH concentrations (C_i) ranging between 0.05 and $0.65 \mu\text{mol L}^{-1}$.
144 Previously, it was determined that equilibrium was reached in $< 24 \text{ h}$ and that no measurable
145 degradation occurred during this period. Initial PAH solutions without adsorbent were also
146 shaken for 24 h and served as controls to account for losses of the PAHs due to processes
147 different from adsorption to the solid (volatilization, adsorption to glassware, etc.). After
148 equilibration, the suspensions were centrifuged ($9000 \times g$, 15 min) and 4 mL of the supernatant
149 solution were removed. The PAHs were determined by high performance liquid

150 chromatography (HPLC) as described below, calculating the amount of PAH adsorbed (C_s)
151 from the difference between the initial (C_i) and equilibrium (C_e) solution concentrations:

152

$$153 \quad C_s = [(C_i - C_e) / m] \cdot V \quad (1)$$

154

155 where C_s ($\mu\text{mol kg}^{-1}$) is the amount of PAH adsorbed at the equilibrium concentration C_e (μmol
156 L^{-1}), m is the adsorbent mass (kg) and V is the solution volume (L).

157 Desorption was performed immediately after adsorption from the highest equilibrium point

158 of the adsorption isotherm. The 4 mL of supernatant removed, and used for the adsorption

159 analysis, were replaced with 4 mL of distilled water. After shaking for 24 h at 20 ± 2 °C, the

160 suspensions were centrifuged, and the equilibrium concentrations of the PAHs in the

161 supernatant were determined by HPLC. This desorption procedure was conducted three times.

162 Adsorption–desorption data were fit to the logarithmic form of the Freundlich equation: $\log C_s$

163 $= \log K_f + N_f \log C_e$, where K_f ($\mu\text{mol}^{1-N_f} \text{L}^{N_f} \text{kg}^{-1}$) and N_f (unitless) are the empirical Freundlich

164 constants. Hysteresis coefficients, H , were calculated according to $H = N_{f\text{-des}} / N_f$, where N_f and

165 $N_{f\text{-des}}$ are the Freundlich slopes of the adsorption and desorption isotherms, respectively [25].

166

167 *2.4. PAHs adsorption by unamended and organo/LDH-amended soil*

168 Triplicate samples (100 mg) of soil were amended with HT-DDS at different rates (0%, 4%

169 and 10%) in order to evaluate its effect on PAHs adsorption compared with unamended soil

170 samples. The mixture was homogenized and 10 mL of an aqueous solution containing the six

171 PAHs selected at $C_i = 50 \mu\text{g L}^{-1}$ each was added. PAHs adsorption was measured using the

172 batch equilibration procedure by stirring the samples for 24 h at 20 ± 2 °C, after which they

173 were centrifuged at 4000 rpm for 20 min and the amount of PAHs in the supernatant was

174 analyzed by HPLC. Quantification of the adsorbed PAHs was achieved from the difference

175 between the initial concentration (C_i) and the equilibrium solution concentration (C_e), and was

176 expressed as a percentage of the initial concentration (C_i).

177

178 *2.5. Organo/LDH as an immobilizer amendment in a PAH-contaminated soil*

179 The effect of HT-DDS as an amendment to reduce the mobility of PAHs in a previously
180 contaminated soil was studied by means of a desorption experiment in which 100 mg of soil
181 was spiked with 100 mg kg⁻¹ of each PAH, previously dissolved in acetone. The organic solvent
182 was allowed to evaporate afterward for 24 h at room temperature. Then, two different amounts
183 of HT-DDS (4% and 10% w/w) were added to the soil and the mixture was homogenized. Ten
184 mL of distilled water was added to 100 mg of unamended or HT-DDS-amended contaminated
185 soil, shaken at 52 rpm for 24 h at 20 ± 2 °C, centrifuged and analyzed for PAHs content of the
186 supernatant by HPLC. The desorption of PAHs from unamended and HT-DDS-amended soil
187 was compared.

188

189 *2.6. PAHs analysis*

190 Analysis of the PAHs was carried out by HPLC. Chemicals were separated on a Water PAH
191 C-18, S-5 µm, 250 mm x 4.6 mm column, with 50:50 acetonitrile/water to 100% acetonitrile
192 linear gradient, run over 18 min at a flow rate of 1.5 mL min⁻¹. The gradient was produced by a
193 Waters 1525 Binary HPLC Pump. A 20 µL injection volume of PAHs was analyzed by HPLC
194 using a UV detector (Waters 2996 diode-array detector) at 254 nm and a fluorescence detector
195 (Waters 2475 Multi λ fluorescent detector) operating simultaneously in series. All data were
196 processed and stored using the program Empower System designed by Water. External
197 calibration curves with standard solutions of PAHs between 0.1-100 µg L⁻¹ were used in the
198 calculations.

199

200 **3. Results and discussion**

201 *3.1. Characterization of organo/LDH nanohybrid adsorbent*

202 Table 2 shows the elemental analysis results for Mg, Al, C and S for HTCO₃ and HT-DDS,
203 as well as some molar ratios. Chemical compositions indicated that the solids prepared had a
204 Mg/Al ratio of 3.0:1.0, which was the same as in the starting Mg/Al nitrate solution. **The**

205 elemental analysis revealed no detectable amount of N in the samples, indicating lack of NO_3^-
206 ions in the interlayer.

207 The empirical formula of the HTCO_3 sample was derived from its chemical composition. On
208 the basis of the lack of N in the samples, CO_3^{2-} was assumed to be the intercalated anion,
209 whereas the water content was obtained from the mass lost in the corresponding TG-curves (not
210 shown). For HT-DDS, the S/Al molar ratio (S/Al = 1.28), allows to determine the organic anion
211 content, which is higher than that required to compensate the layer charge (S/Al = 1). This
212 phenomenon has also been observed by other authors for Mg-Al hydrotalcites [18,26], and
213 indicates that a number of DDS anions should be associated with sodium ions (or hydrogen
214 ions) to balance the charge. You et al. [18] reported that the excess of surfactant intercalated
215 could be due to non-polar interactions with the hydrophobic alkyl groups of exchanged DDS
216 anions. In fact, the high affinity between DDS and the LDH surface has been confirmed in a
217 previous study on the effect of DDS adsorption on the surface charge characteristics of LDH,
218 where DDS was found to change the positive electrokinetic (ζ) potential values of a Mg-Al-Cl
219 LDH to negative values even at low amounts of adsorbed DDS [27].

220 The PXRD patterns obtained for HTCO_3 , HT-DDS, and HT500 are shown in Fig. 1 and are
221 similar to those previously reported for similar samples [28-30]. The diffractograms of HTCO_3
222 and HT-DDS samples correspond to those typical of hydrotalcite-like compounds with a well-
223 ordered layered structure. The PXRD pattern of HTCO_3 , with the basal spacing of $d_{003} = 7.8 \text{ \AA}$,
224 is characteristic for carbonate as interlayer anion. Several orders of basal (00l) reflections were
225 identified in the diffractogram of HT-DDS between 25.9 and 3.8 \AA , and as expected, they were
226 shifted to higher d_{00l} values ($d_{003} = 25.9 \text{ \AA}$) compared to HTCO_3 , consistent with the successful
227 perpendicular intercalation of the surfactant in an all-trans conformation of the alkyl chains
228 regarding to the brucite-type layer [26]. On the other hand, the diffractogram shown in Fig. 1C
229 corresponds to HTCO_3 calcined at 500°C (HT500), with the diffraction peaks characteristic of
230 an Al and Mg mixed oxide [31].

231 Figure 2 shows the FT-IR spectra of HTCO_3 and HT-DDS, as well as the spectrum of the
232 dodecylsulfate sodium salt (Fig. 2B), which was recorded as a reference. As expected, the

233 infrared spectra of HTCO₃ (Fig. 2A) and HT-DDS (Fig. 2C) show the characteristic absorption
234 bands according to the hydrotalcite structure and composition. Besides a broad band centered at
235 3500 cm⁻¹ due to the stretching mode $\nu_{\text{O-H}}$ of hydration water molecules and OH-groups of the
236 brucite-like layers, we observed a weak peak at 1640 cm⁻¹ corresponding to the H₂O water
237 bending mode ($\delta_{\text{O-H}}$) of the interlayer water molecules. The bands in the range of 500-800 cm⁻¹
238 can be assigned to metal-oxygen lattice vibration, suggesting the formation of Mg-Al hydroxide
239 layers.

240 For HTCO₃, the band at 1370 cm⁻¹ confirms the presence of intercalated CO₃²⁻ (ν_{CO_3}) [5].
241 The presence of DDS anions in the organo/LDH (HT-DDS) is evidenced by the triplet observed
242 in the 2850-2965 cm⁻¹ region, due to the C-H stretching vibration ν_{CH_3} bands (2958, 2919 and
243 2851 cm⁻¹), and the C-H bending vibration band $\delta_{\text{C-H}}$ at 1469 cm⁻¹. In addition, bands due to
244 antisymmetric (doublet at 1246 and 1224 cm⁻¹) and symmetric (1066 cm⁻¹) sulfate S=O
245 stretching vibration ($\nu_{\text{S=O}}$) were also observed [15,26].

246

247 3.2. Adsorption-desorption isotherms

248 Figure 3 shows the adsorption isotherms of the six PAHs on HT-DDS. The PAHs adsorption
249 on the inorganic samples HTCO₃ and HT500 was very low (data not included), as has been
250 observed for other non-polar organic compounds [16]. The adsorption parameters of the PAHs
251 on HT-DDS were obtained by fitting the adsorption isotherms to the Freundlich model, and the
252 parameters are summarized in Table 3. **Determination of Freundlich constants was not possible**
253 **in cases where adsorption was close to 100% (phenanthrene, fluoranthene, and pyrene) or in**
254 **cases of very low adsorption (HTCO₃ and HT500).** Adsorption isotherms, along with K_f values,
255 showed the greater affinity of the PAHs for HT-DDS than for HTCO₃ and its calcined product
256 (HT500), which could be attributed to hydrophobic interactions between the PAHs and the alkyl
257 chains of the DDS anions. This result is very similar to that previously reported for the
258 adsorption of the herbicides carbetamide, metamitron and terbuthylazine by the same adsorbents
259 [16,32]. This behavior confirmed that the transformation of the nanocomposite surface nature

260 from hydrophilic to hydrophobic increases its affinity for hydrophobic compounds, such as
261 PAHs, by adsolubilization mechanisms [16,19].

262 The adsorption of the PAHs by HT-DDS increased with the molecular weight of the
263 compound, reaching up to 100% for fluoranthene and pyrene at all concentrations tested.
264 Isotherms and N_f values, close to unity, indicated linear or C-type adsorption according to the
265 classification of Giles et al. [33]. This type of isotherms characterize systems with a minimum
266 competition between the solute and the solvent for adsorption sites of the adsorbent, reflecting a
267 constant partition mechanism, in this case through hydrophobic-type interactions into the bulk
268 state of the interlayer organic phase [34]. Moreover, C-type isotherms are very common for the
269 adsorption of very hydrophobic organic compounds, whose concentration is limited by their low
270 water solubility.

271 Desorption curves showed very high hysteresis in most cases, revealing a great irreversibility
272 of the adsorption process. This agrees with the low values of H coefficient (N_{f-des}/N_{f-ads}) found
273 in those cases where its calculation was possible. Otherwise, these results also confirmed the
274 very high affinity of the PAHs to HT-DDS, where once adsorbed, water is not able to reach the
275 adsorption sites where PAHs remain retained [35]. This may be interesting from the point of
276 view of the applicability of these nanomaterials as adsorbents of PAHs as a water
277 decontamination strategy.

278

279 *3.3. PAHs adsorption by unamended and HTDDS-amended soil samples*

280 Since HT-DDS displayed good adsorbent properties for the PAHs, we studied its application
281 as an amendment to increase the adsorption capacity of a typical Mediterranean soil. The soil
282 was chosen because of its physicochemical characteristics, with a coarse texture and low
283 organic matter content resulting in a high-risk leaching potential for chemicals like the PAHs
284 studied. Figure 4 shows the results of the PAHs adsorption to the Mediterranean soil,
285 unamended and amended with different amounts of HT-DDS (4% and 10% w/w). Adsorption of
286 non-polar organic compounds strongly depends on the organic carbon (OC) content in soil or
287 sediment [36,37]. In this case, the soil presents a low capacity of adsorption for the lower

288 molecular weight PAHs, probably due to its low organic matter content. Adsorption increased
289 with the hydrophobicity of the PAHs and their molecular weight (from acenaphthene: ~ 13%, to
290 pyrene: ~ 60 %, Table 1), with a very good correlation between $\log K_{ow}$ and $\log K_d$ (Fig. 5),
291 which suggests the dominance of nonspecific interactions (van der Waals forces) in the
292 adsorption mechanism of these compounds [38].

293 The application of HT-DDS to the soil increased its adsorption properties for the six PAHs.
294 The increase in adsorption was particularly high for the more hydrophilic PAHs as a result of
295 the low affinity of these PAHs for the unamended soil (Fig. 4). It is noticeable that the increase
296 in adsorption depended on the amount of organo/LDH added. However, the differences found in
297 the PAH adsorption after increasing the amount of nanocomposite added to the soil, from 4% to
298 10%, was not so important. This could be due to the high affinity of the nanocomposite for the
299 PAHs and the high amount of amendment used. Consequently, the percentage of amendment is
300 a parameter that must be optimized from the point of view of the adsorption efficiency.

301 In order to compare the effectiveness of HT-DDS in adsorbing the PAHs in the presence of
302 soil, the experimentally measured adsorption constants, K_{d-meas} , for PAHs on the amended soil
303 were compared with the expected values, K_{d-calc} (Table 4). The expected values were calculated
304 assuming linear and independent adsorption behavior of both systems, soil and HT-DDS, using
305 the following equation:

306

$$307 \quad K_{d-calc} = \theta_{soil} K_{d-soil} + \theta_{HT-DDS} K_{d-HTDDS} \quad (2)$$

308

309 where K_{d-soil} and $K_{d-HTDDS}$ are the distribution coefficients for PAHs adsorption on soil and HT-
310 DDS, respectively, and θ_{soil} and θ_{HT-DDS} are the respective mass fractions of soil and HT-DDS in
311 the mixture [39-41].

312 The results show that the adsorption of PAHs by the soil increased after its amendment with
313 HT-DDS, being the values of the experimental adsorption coefficients for the mixtures close to
314 those expected (Table 4). Unlike previous findings with organoclays for adsorbing polar non-
315 ionic pesticides [39], the presence of soil components resulted in little competition for

316 adsorption sites and the nanocomposite maintained the performance in adsorbing PAHs. It
317 should be noted that acenaphthene did not meet the prerequisite of linearity ($N_f = 1$) required to
318 use Eq. 2 (Table 3), whereas for fluoranthene and pyrene the calculation of K_d values was not
319 possible because of the complete adsorption of both PAHs by the nanocomposite.

320 In order to compare the effectiveness of the organic C of soil and HTDDS in adsorbing the
321 PAHs, the K_d values at $C_i = 50 \mu\text{g L}^{-1}$ were normalized to the organic C content of the different
322 samples. As shown in Table 3, C-normalized K_d constants, K_{d-oc} , for HTDDS became at least ten
323 times higher than that of the soil (Table 4). This result indicates enhanced interaction of PAHs
324 with HTDDS compared to the soil, with regard to their organic C contents, and higher
325 efficiency of HT-DDS as an adsorbent of PAHs.

326

327 *3.4. Effect of HTDDS addition on PAHs desorption from a previously contaminated soil*

328 Figure 6 shows the amount of PAH desorbed from the polluted soil, either unamended or
329 amended with HT-DDS at two different rates (4% and 10% w/w). The amount of PAH desorbed
330 from the amended soil was referenced to the amount of PAH desorbed from the unamended
331 soil. The addition of HT-DDS to the soil improved the immobilization of the PAHs, with a
332 decrease in the amount of PAH desorbed from the soil ranging from 70 to 95% under the
333 experimental conditions tested. For unamended soil, the concentrations of desorbed PAHs
334 ranged between ca. $800 \mu\text{g L}^{-1}$ (acenaphthene) and $60 \mu\text{g L}^{-1}$ (anthracene). For HTDDS-
335 amended soil, the concentrations of desorbed PAHs were in all cases less than $50 \mu\text{g L}^{-1}$. They
336 ranged between $48 \mu\text{g L}^{-1}$ (acenaphthene) and ca. $7 \mu\text{g L}^{-1}$ (pyrene) for soil amended with
337 HTDDS at 4%, and between ca. $40 \mu\text{g L}^{-1}$ (acenaphthene) and $3 \mu\text{g L}^{-1}$ (pyrene) for soil
338 amended with HTDDS at 10%.

339 The increase in PAHs retention depended on the amount of HT-DDS added, although
340 increasing the amendment rate from 4% to 10% resulted in little improvement in PAH
341 immobilization. Therefore, the amendment rate is a parameter that should be optimized, since
342 further addition of HT-DDS does not necessarily involve a significant improvement in the soil
343 capability to immobilize the PAHs.

344 The results show that the addition of HT-DDS, used as an adsorbent material, could be a
345 strategy for immobilizing hydrophobic organic compounds such as PAHs. Organo/LDH
346 materials could be used as amendments or barriers emplaced in soils polluted with non-ionic
347 organic compounds to reduce their mobility and, therefore, to prevent the pollution of
348 environmental compartments adjacent to that zone, even enabling the natural degradation of
349 these compounds in situ.

350

351 **4. Conclusions**

352 Our results show that the successfully synthesized organo/LDH (HT-DDS) presents higher
353 affinity for the adsorption of hydrophobic compounds such as the six PAHs selected
354 (acenaphthene, fluorene, phenanthrene, anthracene, fluoranthene and pyrene) compared with
355 inorganic hydrotalcite (HTCO_3) and its calcined product (HT500), with a great irreversibility of
356 the adsorption process. These results are consistent with the hypothesis that the transformation
357 of the nature of the hydrotalcite surface from hydrophilic to hydrophobic increases its affinity
358 for very hydrophobic organic compounds. On the other hand, our experiments testing the
359 HTDDS nanocomposite as an immobilizer or barrier for PAHs in soil show that the amount of
360 PAH adsorbed in HTDDS-amended soil depends on the amount of HTDDS applied, as well as
361 on the nature of the PAH. The adsorption of PAHs in HTDDS-amended soil increases as
362 expected according to an independent adsorption behavior of both systems: soil-water and
363 HTDDS-water. Significant correlations were found between logarithmic values of K_{ow} and K_d ,
364 suggesting nonspecific interactions in the adsorption mechanism of the PAHs. By normalizing
365 adsorption coefficient K_d to the organic C content, HTDDS revealed more efficient properties as
366 an adsorbent compared to the soil. Therefore, the nanocomposite HTDDS can also be used as an
367 amendment or barrier of contaminated soils as a strategy to enhance the soil retention capacity
368 of PAHs and to decrease their mobility.

369

370

371

372 **Acknowledgments**

373 This work was financed by the Spanish Government through Project 300/PC/08/3-01.2 of
374 Ministerio de Medio Ambiente y Medio Rural y Marino, Junta de Andalucía through Research
375 Group AGR-264, and the European Union through Project PIRSES-GA-2008-230796 and
376 FEDER funds (Operative Program 2007-2013). The authors thank I. Guzman for technical
377 assistance.

378

379 **References**

- 380 [1] A.K. Haritash, C.P. Kaushik, Biodegradation aspects of Polycyclic Aromatic Hydrocarbons
381 (PAHs): A review, *J. Hazard. Mater.* 169 (2009) 1-15.
- 382 [2] R. Posada-Baquero, J.J. Ortega-Calvo, Recalcitrance of polycyclic aromatic hydrocarbons
383 in soil contributes to background pollution, *Environ. Pollut.* 159 (2011) 3692-3699.
- 384 [3] U. Ghosh, R.G. Luthy, G. Cornelissen, D. Werner, C.A. Menzie, In-situ sorbent
385 amendments: A new direction in contaminated sediment management, *Environ. Sci.*
386 *Technol.* 45 (2011) 1163-1168.
- 387 [4] D. Mohan, J. Pittman, Activated carbons and low cost adsorbents for remediation of tri-
388 and hexavalent chromium from water, *J. Hazard. Mater.* 137 (2006) 762-811.
- 389 [5] F. Cavani, F. Trifirò, A. Vaccari, Hydrotalcite-type anionic clays: Preparation, properties
390 and applications, *Catalysis Today* 11 (1991) 173-301.
- 391 [6] J. Cornejo, R. Celis, I. Pavlovic, M.A. Ulibarri, Interactions of pesticides with clays and
392 layered double hydroxides: a review, *Clay Miner.* 43 (2008) 155-175.
- 393 [7] I. Pavlovic, M.A. Ulibarri, M.C. Hermosín, J. Cornejo, Sorption of an anionic surfactant
394 from water by a calcined hydrotalcite-like sorbent, *Fresenius Environ. Bull.* 6 (1997) 266-
395 271.

- 396 [8] J. Villaverde, C. Maqueda, T. Undabeytia, E. Morillo, Effect of various cyclodextrins on
397 photodegradation of a hydrophobic herbicide in aqueous suspensions of different soil
398 colloidal components, *Chemosphere* 69 (2007) 575-584.
- 399 [9] M. Meyn, K. Beneke, G. Lagaly, Anion-exchange reactions of layered double hydroxides,
400 *Inorg. Chem.* 29 (1990) 5201-5207.
- 401 [10] V. Rives, *Layered Double Hydroxides: Present and Future*, Nova Science Publishers, Inc.,
402 New York, 2002.
- 403 [11] M.C. Hermosín, I. Pavlovic, M.A. Ulibarri, J. Cornejo, Trichlorophenol adsorption on
404 layered double hydroxide: A potential sorbent, *J. Environ. Sci. Health Part A Environ. Sci.*
405 *Eng.* 28 (1993) 1875-1888.
- 406 [12] R. Celis, W.C. Koskinen, A.M. Cecchi, G.A. Bresnahan, M.J. Carrisoza, M.A. Ulibarri, I.
407 Pavlovic, M.C. Hermosín, Sorption of the ionizable pesticide imazamox by organo-clays
408 and organohydrotalcites, *J. Environ. Sci. Health Part B Pestic. Food Contamin. Agric.*
409 *Wastes* 34 (1999) 929-941.
- 410 [13] J. Inacio, G. Taviot, C. Forano, J.P. Besse, Adsorption of MCPA pesticide by MgAl-
411 layered double hydroxides, *Appl. Clay Sci.* 18 (2001) 255-264.
- 412 [14] L.P. Cardoso, J.B. Valim, Study of acids herbicides removal by calcined Mg-Al-CO₃-
413 LDH, *J. Phys. Chem. Solids* 67 (2006) 987-993.
- 414 [15] M. Bouraada, F. Belhafaoui, M.S. Ouali, L.C. de Ménorval, Sorption study of an acid dye
415 from an aqueous solution on modified Mg-Al layered double hydroxides, *J. Hazard. Mater.*
416 163 (2009) 463-467.
- 417 [16] F. Bruna, I. Pavlovic, C. Barriga, J. Cornejo, M.A. Ulibarri, Adsorption of pesticides
418 Carbetamide and Metamitron on organohydrotalcite, *Appl. Clay Sci.* 33 (2006) 116-124.

- 419 [17] M.A. Ulibarri, I. Pavlovic, M.C. Hermosín, J. Cornejo, Hydrotalcite-like compounds as
420 potential sorbents of phenols from water, *Appl. Clay Sci.* 10 (1995) 131-145.
- 421 [18] Y. You, H. Zhao, G.F. Vance, Surfactant-enhanced adsorption of organic compounds by
422 layered double hydroxides, *Colloids Surf. A Physicochem. Eng. Asp.* 205 (2002) 161-172.
- 423 [19] Y.H. Chuang, C.H. Liu, Y.M. Tzou, J.S. Chang, P.N. Chiang, M.K. Wang, Comparison
424 and characterization of chemical surfactants and bio-surfactants intercalated with layered
425 double hydroxides (LDHs) for removing naphthalene from contaminated aqueous
426 solutions, *Colloids Surf. A Physicochem. Eng. Asp.* 366 (2010) 170-177.
- 427 [20] D. Mackay, W.Y. Shiu, Aqueous solubility of polynuclear aromatic hydrocarbons, *J.*
428 *Chem. Eng. Data* 22 (1977) 399-402.
- 429 [21] G.N. Lu, X.Q. Tao, Z. Dang, X.Y. Yi, C. Yang, Estimation of *n*-octanol/water partition
430 coefficients of polycyclic aromatic hydrocarbons by quantum chemical descriptors, *Cent.*
431 *Eur. J. Chem.* 6 (2008) 310-318.
- 432 [22] C.T. Chiou, S.E. McGroddy, D.E. Kile, Partition characteristics of polycyclic aromatic
433 hydrocarbons on soils and sediments, *Environ. Sci. Technol.* 32 (1998) 264-269.
- 434 [23] K.C. Jones, J.A. Stratford, K.S. Waterhouse, N.B. Vogt, Organic contaminants in welsh
435 soils: Polynuclear aromatic hydrocarbons, *Environ. Sci. Technol.* 23 (1989) 540-550.
- 436 [24] W.T. Reichle, Synthesis of anionic clay minerals (mixed metal hydroxides, hydrotalcite),
437 *Solid State Ion.* 22 (1986) 135-141.
- 438 [25] E. Barriuso, D.A. Laird, W.C. Koskinen, R.H. Dowdy, Atrazine desorption from smectites,
439 *Soil Sci. Soc. Am. J.* 58 (1994) 1632-1638.
- 440 [26] A. Clearfield, M. Kieke, J. Kwan, J.L. Colon, R.C. Wang, Intercalation of dodecyl-sulfate
441 into layered double hydroxides, *J. Incl. Phenom. Mol. Recog. Chem.* 11 (1991) 361-378.

- 442 [27] R. Rojas, F. Bruna, C.P. de Pauli, M.A. Ulibarri, C.E. Giacomelli, The effect of interlayer
443 anion on the reactivity of Mg-Al layered double hydroxides: Improving and extending the
444 customization capacity of anionic clays, *J. Colloid Interface Sci.* 359 (2011) 136-141.
- 445 [28] P.C. Pavan, E.L. Crepaldi, J.B. Valim, Sorption of anionic surfactants on layered double
446 hydroxides, *J. Colloid Interface Sci.* 229 (2000) 346-352.
- 447 [29] E.L. Crepaldi, P.C. Pavan, J. Tronto, J.B. Valim, Chemical, structural, and thermal
448 properties of Zn(II)-Cr(III) layered double hydroxides intercalated with sulfated and
449 sulfonated surfactants, *J. Colloid Interface Sci.* 248 (2002) 429-442.
- 450 [30] T. Kameda, M. Saito, Y. Umetsu, Preparation of a composite material for the uptake of
451 bisphenol A from aqueous solutions, the dodecylsulfate ion-intercalated Mg-Al layer-
452 structured double hydroxide particles, *J. Alloy Compd.* 402 (2005) 46-52.
- 453 [31] F.M. Labajos, V. Rives, M.A. Ulibarri, Effect of hydrothermal and thermal treatments on
454 the physicochemical properties of Mg-Al hydrotalcite-like materials, *J. Mater. Sci.* 27
455 (1992) 1546-1552.
- 456 [32] F. Bruna, I. Pavlovic, R. Celis, C. Barriga, J. Cornejo, M.A. Ulibarri, Organohydrotalcites
457 as novel supports for the slow release of the herbicide terbuthylazine, *Appl. Clay Sci.* 42
458 (2008) 194-200.
- 459 [33] C.H. Giles, T.H. MacEwan, S.N. Nakhwa, D. Smith, Studies in adsorption. Part XI. A
460 system of classification of solution adsorption isotherms, and its use in diagnosis of
461 adsorption mechanisms and in measurement of specific surface areas of solids, *J. Chem.*
462 *Soc.* (1960) 3973-3993.
- 463 [34] C.T. Chiou, P.E. Porter, D.W. Schmedding, Partition equilibria of nonionic organic
464 compounds between soil organic matter and water, *Environ. Sci. Technol.* 17 (1983) 227-
465 231.

- 466 [35] R. Celis, J. Cornejo, M.C. Hermosín, W.C. Koskinen, Sorption-desorption of atrazine and
467 simazine by model soil colloidal components, *Soil Sci. Soc. Am. J.* 61 (1997) 436-443.
- 468 [36] C.T. Chiou, Partition and adsorption of organic contaminants in environmental system,
469 John Wiley & Sons, New York, 2002.
- 470 [37] S.W. Karickhoff, D.S. Brown, T.A. Scott, Sorption of hydrophobic pollutants on natural
471 sediments, *Water Res.* 13 (1979) 241-248.
- 472 [38] E. Bi, T.C. Schmidt, and S.B. Haderlein, Sorption of heterocyclic organic compounds to
473 reference soils: column studies for process identification, *Environ. Sci. Technol.* 40 (2006)
474 5962-5970.
- 475 [39] B. Gámiz, R. Celis, M.C. Hermosín, J. Cornejo, Organoclays as soil amendments to
476 increase the efficacy and reduce the environmental impact of the herbicide fluometuron in
477 agricultural soils, *J. Agric. Food Chem.* 58 (2010) 7893-7901.
- 478 [40] M.S. Rodríguez-Cruz, M.J. Sánchez-Martín, M.S. Andrades, M. Sánchez-Carmanzano,
479 Modification of clay barriers with a cationic surfactant to improve the retention of
480 pesticides in soils, *J. Hazard. Mater.* 139 (2007) 363-372.
- 481 [41] E.A. Voudrias, The concept of a sorption chemical barrier for improving effectiveness of
482 landfill liners, *Waste Manage.* 20 (2002) 251-258.
483
484

Legends to the figures

485

486

487 **Fig. 1.** PXRD patterns for the samples A) HTCO_3 , B) HT-DDS and C) HT500. (* diffraction
488 peaks due to the Al sample holder).

489

490 **Fig. 2.** FT-IR spectra of A) HTCO_3 , B) DDS and C) HT-DDS.

491

492 **Fig. 3.** PAHs adsorption (solid symbol) – desorption (open symbol) isotherms on HT-DDS.

493

494 **Fig. 4.** PAH adsorption by unamended and HT-DDS-amended soil (4% or 10%) at an initial
495 PAH concentration of $50 \mu\text{g L}^{-1}$.

496

497 **Fig. 5.** Relationship between $\log K_{ow}$ and $\text{Log } K_d$ in unamended soil at an initial concentration of
498 $50 \mu\text{g L}^{-1}$ of each PAH.

499

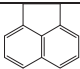
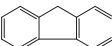
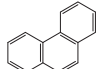
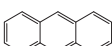
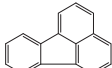

500 **Fig. 6.** Percentage of PAH desorbed from the organo/LDH-amended soil (4 or 10% w/w),
501 referenced to the amount desorbed from unamended soil.

502

503

Table 1

Molecular structure and physicochemical properties of the PAHs.

Molecule	Molecular structure	MW (g mol ⁻¹)	Water solubility ^a	
			(mg L ⁻¹)	log <i>K</i> _{ow}
Acenaphthene		154.2	3.93	3.92 ^b
Fluorene		166.2	1.98	4.18 ^b
Phenanthrene		178.0	1.29	4.57 ^{b, c}
Anthracene		178.0	0.07	4.54 ^b
Fluoranthene		202.0	0.26	5.22 ^b
Pyrene		202.0	0.14	5.18 ^c

^a Solubility in water (25°C), [20].^b From reference [21]^c From reference [22].

Table 2

Chemical composition of adsorbents and proposed formulae.

Sample	Weight (%)				Atomic ratio			Proposed Formulae
	Mg	Al	C	S	S/Al	C/Al	Mg/Al	
HTCO ₃	23.8	8.8	2.3	-	-	1.30	3.04	Mg _{3.0} Al(OH) ₈ (CO ₃) _{0.5} · 2.8 H ₂ O
HT-DDS	10.8	4.0	29.6	6.1	1.28	16.70	3.00	[Mg _{3.0} Al(OH) ₈ (DDS) _{1.00} ·2.6 H ₂ O] (NaDDS) _{0.28}

Table 3

Freundlich model parameters for PAH adsorption on HT-DDS, hysteresis coefficient (H) and organic C-normalized K_d values (K_{d-oc} ; L g⁻¹).

Adsorbent	Molecule	K_f	N_f	R^2	H	K_{d-oc}^b
HT-DDS	Acenaphthene	3.96 (2.05 - 7.66) ^a	0.76 ± 0.12	0.98	0.13	40
	Fluorene	18.20 (14.64- 22.70)	0.99 ± 0.04	0.99	0.10	62
	Phenanthrene	-	-	-	-	194
	Anthracene	70.41 (55.41 - 89.46)	0.99 ± 0.03	0.99	0.01	239
	Fluoranthene	-	-	-	-	-
	Pyrene	-	-	-	-	-

^a Standard error.

^b K_{d-oc} at $C_i = 50 \mu\text{g L}^{-1}$.

Table 4

Measured and calculated distribution coefficients K_d ($L\ g^{-1}$) for PAHs adsorption on unamended and organo/LDH-amended soil, and the organic C-normalized K_d values (K_{d-oc} ; $L\ g^{-1}$).

PAH	Treatment	K_{d-meas}	K_{d-calc}	K_{d-oc}
Acenaphthene	Unamended	< 0.1		2.9
	HT-DDS 4%	0.8 ± 0.3	0.5	
	HT-DDS 10%	1.0 ± 0.0	1.2	
Fluorene	Unamended	< 0.1		3.8
	HT-DDS 4%	1.0 ± 0.4	0.8	
	HT-DDS 10%	1.7 ± 0.2	1.9	
Phenanthrene	Unamended	< 0.1		7.6
	HT-DDS 4%	2.7 ± 0.6	2.3	
	HT-DDS 10%	5.3 ± 0.6	5.7	
Anthracene	Unamended	< 0.1		10.5
	HT-DDS 4%	3.2 ± 0.7	2.9	
	HT-DDS 10%	6.1 ± 0.1	7.1	
Fluoranthene	Unamended	0.13 ± 0.05		24.4
	HT-DDS 4%	-	-	-
	HT-DDS 10%	-	-	-
Pyrene	Unamended	0.15 ± 0.05		29.4
	HT-DDS 4%	-	-	-
	HT-DDS 10%	-	-	-

Figure 1

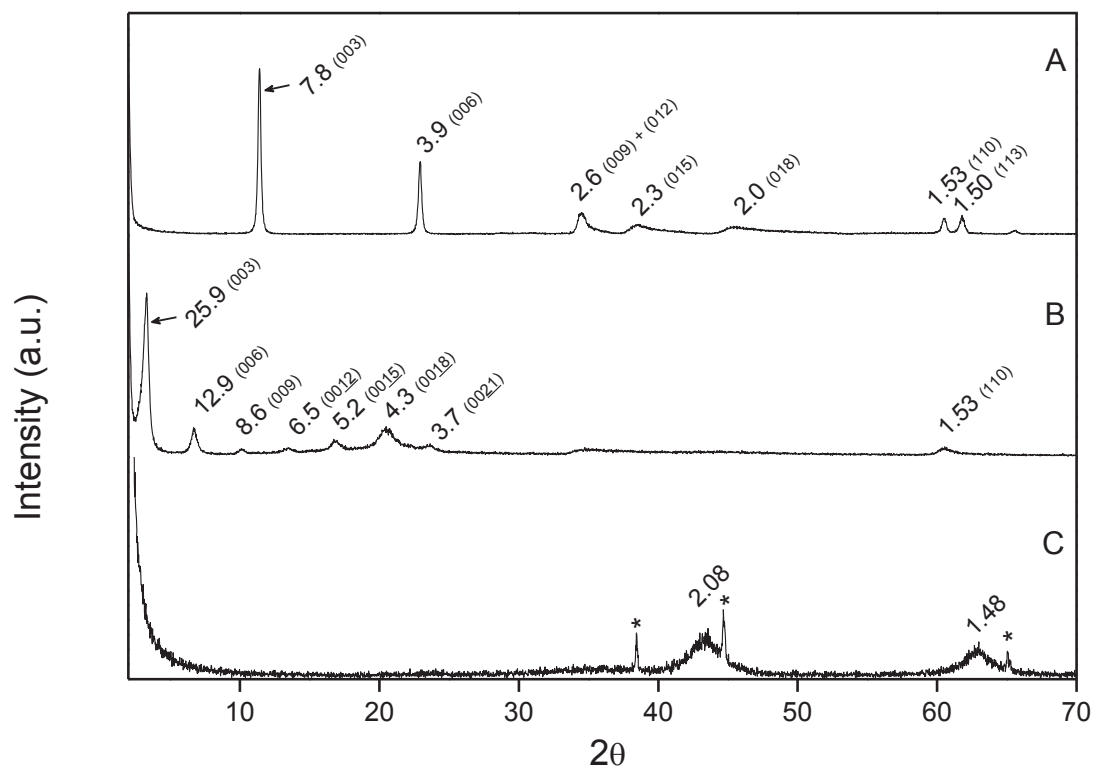


Figure 1. PXRD patterns for the samples A) HTCO₃, B) HT-DDS and C) HT500. (* diffraction peaks due to the Al sample holder)

Figure 2

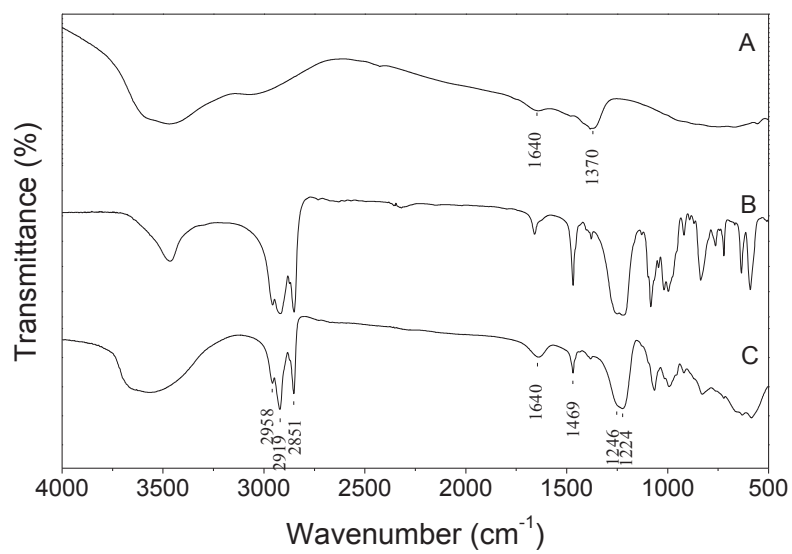


Figure 2. FT-IR spectra of A) HTCO₃, B) DDS and C) HT-DDS.

Figure 3

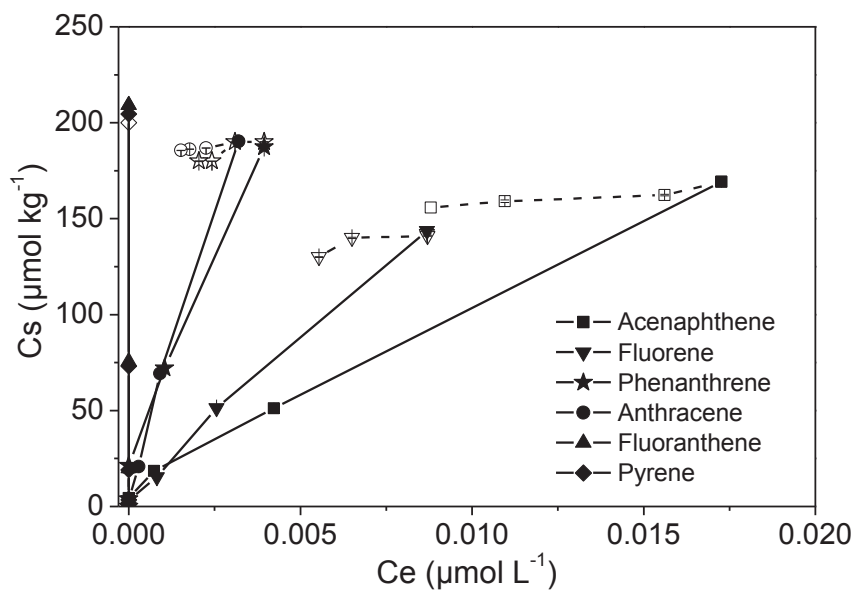


Figure 3. PAHs adsorption (solid symbol) – desorption (open symbol) isotherms on HT-DDS.

Figure 4

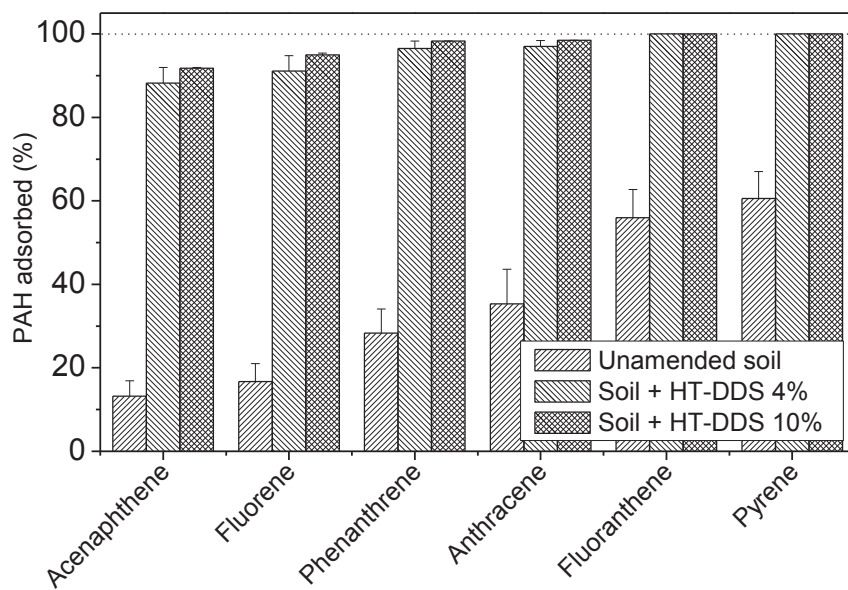


Figure 4. PAH adsorption by unamended and HT-DDS-amended soil (4% or 10%) at an initial PAH concentration of $50 \mu\text{g L}^{-1}$.

Figure 5

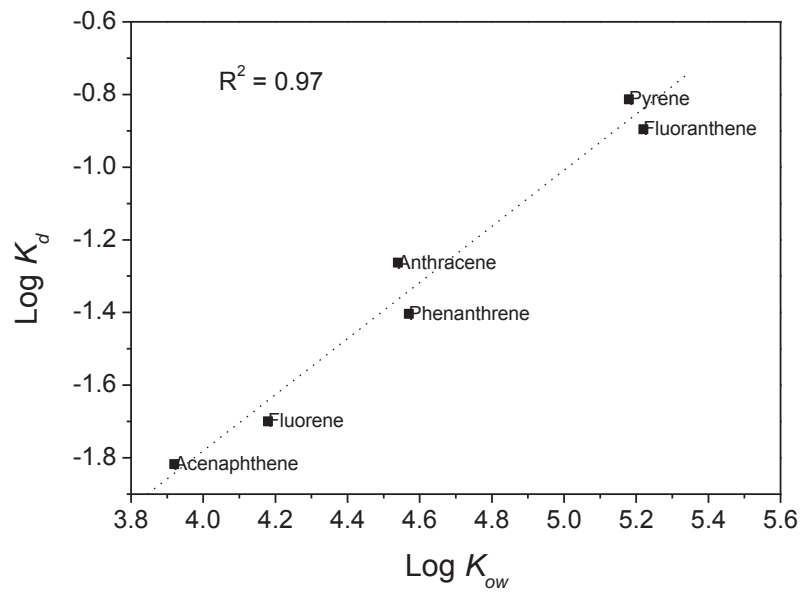


Figure 5. Relationship between $\log K_{ow}$ and $\log K_d$ in unamended soil at an initial concentration of $50 \mu\text{g L}^{-1}$ of each PAH.

Figure 6

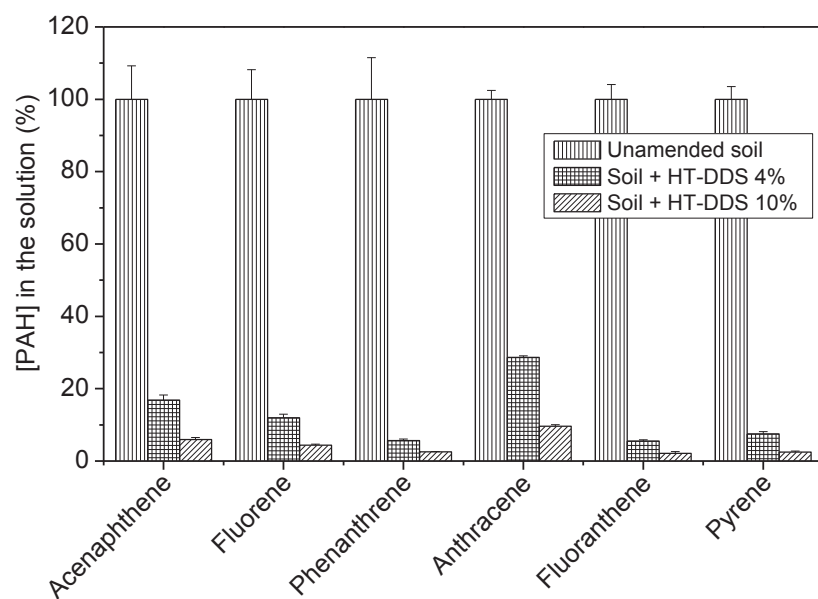


Figure 6. Percentage of PAH desorbed from the organo/LDH-amended soil (4 or 10% w/w), referenced to the amount desorbed from unamended soil.